



HAL
open science

Streamwise bars in fish-friendly angled trashracks

Sylvain Raynal, Ludovic Chatellier, Dominique Courret, Michel Larinier,
Laurent David

► **To cite this version:**

Sylvain Raynal, Ludovic Chatellier, Dominique Courret, Michel Larinier, Laurent David. Streamwise bars in fish-friendly angled trashracks. *Journal of Hydraulic Research*, 2014, vol. 52 (n° 3), pp.426-431. 10.1080/00221686.2013.879540 . hal-01116497

HAL Id: hal-01116497

<https://hal.science/hal-01116497>

Submitted on 13 Feb 2015

HAL is a multi-disciplinary open access archive for the deposit and dissemination of scientific research documents, whether they are published or not. The documents may come from teaching and research institutions in France or abroad, or from public or private research centers.

L'archive ouverte pluridisciplinaire **HAL**, est destinée au dépôt et à la diffusion de documents scientifiques de niveau recherche, publiés ou non, émanant des établissements d'enseignement et de recherche français ou étrangers, des laboratoires publics ou privés.



Open Archive TOULOUSE Archive Ouverte (OATAO)

OATAO is an open access repository that collects the work of Toulouse researchers and makes it freely available over the web where possible.

This is an author-deposited version published in : <http://oatao.univ-toulouse.fr/>
Eprints ID : 11857

To link to this article :

DOI:10.1080/00221686.2013.879540

URL : <http://dx.doi.org/10.1080/00221686.2013.879540>

To cite this version :

Raynal, Sylvain and Chatellier, Ludovic and Courret, Dominique and Larinier, Michel and David, Laurent *Streamwise bars in fish-friendly angled trashracks*. (2014) Journal of Hydraulic Research, vol. 52 (n° 3). pp. 426-431. ISSN 0022-1686

Any correspondence concerning this service should be sent to the repository administrator: staff-oatao@listes-diff.inp-toulouse.fr

Technical note

Streamwise bars in fish-friendly angled trashracks

SYLVAIN RAYNAL, Research Engineer, *Axe HydEE (Hydrodynamique et Ecoulements Environnementaux), Institut P', CNRS – Université de Poitiers – ENSMA, UPR 3346, SP2MI – Téléport 2, 11 Boulevard Marie et Pierre Curie, BP 30179, 86962*

FUTUROSCOPE Chasseneuil Cedex, France

Email: sylvain.raynal@univ-poitiers.fr (author for correspondence)

LUDOVIC CHATELLIER, Assistant Professor, *Axe HydEE (Hydrodynamique et Ecoulements Environnementaux), Institut P', CNRS – Université de Poitiers – ENSMA, UPR 3346, SP2MI – Téléport 2, 11 Boulevard Marie et Pierre Curie, BP 30179, 86962*

FUTUROSCOPE Chasseneuil Cedex, France

Email: ludovic.chatellier@univ-poitiers.fr

DOMINIQUE COURRET, Environmental Engineer, *Pôle Écohydraulique ONEMA – IMFT – IRSTEA, Institut de Mécanique des Fluides de Toulouse, 2 Allée du Professeur Camille Soula, 31400 Toulouse, France*

Email: dcourret@imft.fr

MICHEL LARINIER, Senior Environmental Engineer, *22 Impasse Leonard-André Bonnet, 12100 Millau, France*

Email: michel.larinier@wanadoo.fr

LAURENT DAVID (IAHR Member), Professor, *Axe HydEE (Hydrodynamique et Ecoulements Environnementaux), Institut P', CNRS – Université de Poitiers – ENSMA, UPR 3346, SP2MI – Téléport 2, 11 Boulevard Marie et Pierre Curie, BP 30179, 86962*

FUTUROSCOPE Chasseneuil Cedex, France

Email: laurent.david@univ-poitiers.fr

ABSTRACT

Experimental results for fish-friendly trashracks placed in an open-water channel are presented. Eighteen angled trashracks were used to test different bar spacings, bar shapes and rack angles. Each model trashrack comprised two horizontal supports with regularly spaced slots adjusted to compensate for the trashrack angle, i.e. maintain the vertical bars “streamwise” (parallel to flow). Water depths and velocity profiles were acquired upstream and downstream of each rack configuration. The results reveal that the head-loss coefficient for angled racks with streamwise bars does not depend on the rack angle and can be calculated with equations for racks perpendicular to the channel. Upstream velocity profiles along the rack are not significantly affected by the rack angle and downstream transverse profiles are nearly uniform. A comparison with conventional angled trashracks with bars set perpendicular to the rack revealed the many advantages of streamwise bars.

Keywords: Angled trashrack; downstream migration; head loss; streamwise bars; velocity distribution

1 Introduction

In Europe, the Water Framework Directive (2000/60/EC) and the Council Regulation (1100/2007) for the recovery of eel stocks address the issue of passage through hydraulic turbines causing harm to diadromous fish species, such as European eel, salmon and sea-run brown trout. Passage can be significantly reduced by modifying the bar spacing and the angles of conventional racks at the intakes of hydroelectric power plants

to block fish and guide them towards bypasses located at the downstream end of the rack.

Raynal *et al.* (2013) carried out an experimental study using angled model trashracks with vertical bars set perpendicular to the rack. They first compared their experimental results for head losses with several existing equations. A new equation was proposed that produces more accurate estimates for trashracks with narrow bar spacing and acute angles. It can be decomposed into two main terms, the first for a vertical rack perpendicular to

the channel that includes the influence of the bar shape and the trashrack–blockage ratio, and a second for the effect of the rack angle.

Raynal *et al.* (2013) also focused on velocity distributions and biological criteria. In order to provide a safe, downstream route for fish, velocities along the rack must satisfy two criteria involving the normal V_n and tangential V_t velocity components. The first one related to fish-guidance is defined by $V_t/V_n \geq 1$, whereas the second one aims at avoiding impingement risks with a maximal V_n value of 0.5 ms^{-1} for silver eels and smolts.

These criteria correspond to recommendations given by the French National Agency for Water and Aquatic Environments (ONEMA, Courret and Larinier 2008). Similar ones are also used by other national agencies (OTA 1995, NMFS 2011, Environmental Agency 2012). The results of Raynal *et al.* (2013) showed that, for angled trashracks (herein termed α -PB racks where PB stands for perpendicular bars), the guidance criterion is nearly met for $\alpha = 45^\circ$, but normal velocities V_n are slightly too high in the downstream part of the rack ($V_t/V_n \approx 0.9$). Such velocity behaviour was also measured by Kriewitz *et al.* (2012). Moreover, for $\alpha = 45^\circ$, V_n is close to the approach velocity V_1 at the downstream end of the rack which means that the impingement criterion can be met only when $V_1 \leq 0.5 \text{ ms}^{-1}$, which is very restrictive.

Downstream of the rack, velocity distributions may impact turbine performance. Chatellier *et al.* (2011) carried out velocity measurements with particle image velocimetry (PIV). They revealed an eddying zone along a wall that contrasts with higher velocities along the other wall. Such asymmetry, associated with prohibitive head losses, could significantly lower the overall performance of the installation.

This paper focuses on a new kind of angled rack in which the bars are set parallel to the channel axis (herein termed α -SB racks where SB stands for streamwise bars). Section 2 describes the experimental set-up and presents the main characteristics of the hydraulic installation, the model trashrack and the different measurement devices. Section 3 focuses on head losses

and compares α -PB and α -SB results. A comparison between measured velocity profiles for α -SB racks and α -PB racks is achieved in Section 4 with a specific focus on biological criteria. The results are then discussed in the conclusion and recommendations are made for the design of fish-friendly water intakes using angled racks with streamwise bars.

2 Experimental set-up

The experiments were conducted using model trashracks, inserted in an open channel 10 m long, 0.6 m wide (B) and 0.9 m high. A comparison of α -PB and α -SB rack geometries is illustrated in Fig. 1. The maximum water discharge Q was $0.13 \text{ m}^3 \text{ s}^{-1}$. The water depth, adjusted by a weir at the channel outlet, was set to $H_1 = 0.35 \text{ m}$.

Model trashracks comprised elements scaled down to half size. Two horizontal supports (thickness $D_{sp} = 20 \text{ mm}$) were designed with regularly spaced streamwise slots, in which bars were inserted. Two vertical plates (thickness $b_{ext} = 10 \text{ mm}$) held the supports at each end and served to attach the trashrack to the channel walls. Bars were 5 mm thick (b), 40 mm deep and had either a rectangular (PR) or a more hydrodynamic (PH with a round leading edge and tapered tailing edge) shape (Fig. 1c). They were alternatively spaced at $e = 5, 10$ or 15 mm , reproducing real bar spacings of 10, 20 or 30 mm respectively, with e/b ratios between 1 and 3. These elements determine the trashrack–blockage ratio O_g (Eq. 1) which can be broken down into two variables, one representing the blockage ratio O_b due to the bars and the other the blockage ratio O_{sp} due to the horizontal support. The term $(1 - O_b)$ in the equation for O_{sp} is included to avoid counting twice the zone where the bars and the horizontal support intersect.

$$O_g = O_b + O_{sp} \text{ where } O_b = \frac{N_b b + 2b_{ext}}{B}, O_{sp} = (1 - O_b) \frac{D_{sp}}{H_1} \quad (1)$$

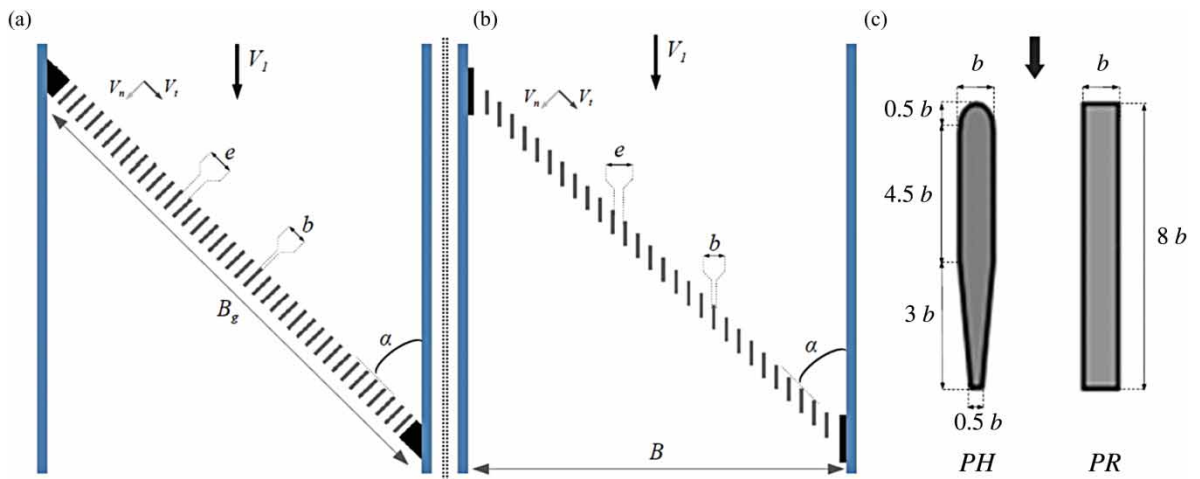


Figure 1 Comparative diagrams for (a) α -PB and (b) α -SB racks. (c) The two bar sections tested (PH and PR) are also detailed

In the above, N_b , b , b_{ext} , B , D_{sp} and H_1 are, respectively, the number of bars, the bar thickness, the thickness of lateral plate, the channel width, the horizontal support thickness and the upstream water depth.

The resulting values of O_g ranged from 0.31 to 0.54. The combination of the various parameters described above and the three trashrack angles tested ($\alpha = 60^\circ, 45^\circ$ and 30°) led to 18 different trashrack configurations.

The discharge Q was measured by an electromagnetic flow meter. Upstream and downstream water depths, respectively, H_1 and H_2 , were measured at $x = -1$ m and $x = 2.6$ m respectively ($x = 0$ m at the upstream end of the rack). Upstream and downstream mean velocities, V_1 and V_2 , respectively, were calculated from Q , H_1 and H_2 .

The head loss due to the rack ΔH (overall uncertainty ≈ 2 mm) was calculated using the Bernoulli equation (Eq. 2) which includes water depths, mean velocities and also the head loss due to the channel ΔH_0 (measured in configurations without a rack). The non-dimensional coefficient ξ was determined for all 18 trashrack configurations.

$$H_1 + \frac{V_1^2}{2g} = H_2 + \frac{V_2^2}{2g} + \Delta H + \Delta H_0, \quad \Delta H = \xi \frac{V_1^2}{2g} \quad (2)$$

Local velocities were measured upstream and downstream of the trashrack with two complementary devices for all 18 configurations. A PIV system produced horizontal velocity maps and was combined with an acoustic Doppler velocimeter (ADV) probe which was moved to acquire velocity profiles. This experimental set-up was similar to that used in Raynal *et al.* (2013) which may be consulted for more detailed information.

3 Trashrack head-loss coefficient

Figure 2 shows, for each bar shape and each bar spacing, the measured head-loss coefficients ξ as a function of α . Head-loss values at $\alpha = 30^\circ, 45^\circ$ and 60° are those measured during this study and values at $\alpha = 90^\circ$ are calculated with the equation proposed in Raynal *et al.* (2013) for vertical racks.

The influence of bar spacing and bar shape on the head-loss coefficient is similar for α -SB and α -PB racks. PH bars generate head losses approximately 40% lower than PR bars and the narrower the bar spacing, the higher the head loss.

On the other hand, the influence of the rack angle α on the head-loss coefficient differs for α -SB and α -PB racks. In each α -SB configuration, ξ remains fairly constant for all α values within the 30-90° range. For α -PB racks (dashed and dotted lines in Fig. 2), ξ increases as α decreases. The fact that α does not influence the head-loss coefficient of α -SB racks means that an equation defined for vertical racks may be used to predict head losses generated by α -SB racks for all α between 30 and 90°. The equation proposed by Raynal *et al.* (2013) for vertical racks

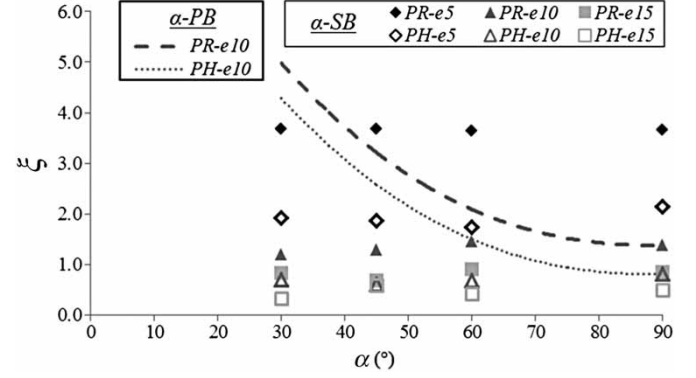


Figure 2 Head-loss coefficient ξ values for α -SB racks (marks) for different bar spacings (model dimensions). Values for $\alpha = 30^\circ, 45^\circ$ and 60° are those measured in this study. The ξ values at $\alpha = 90^\circ$, the dashed line (PR) and the dotted line (PH), illustrating α -PB head-loss coefficients for $e = 10$ mm, are extracted from Raynal *et al.* (2013)

perpendicular to the channel (Eq. 3) may therefore be used to predict head losses

$$\xi = K_i \left(\frac{O_g}{1 - O_g} \right)^{1.6} \quad (3)$$

The value of K_i in Eq. 3 depends on the bar shape and equals 2.89 and 1.7 for PR and PH bars, respectively. On average, measured head-loss coefficients are lower than those predicted with Eq. 3 by only 3.4 and 14.8%, for PR and PH bars, respectively. The largest discrepancies occur for configurations where $e = 15$ mm, for which measurement uncertainties are larger.

Figure 2 also compares head losses for both types of angled racks. At $\alpha = 45^\circ$ and $e = 10$ mm, the streamwise configuration (data points), i.e. α -SB instead of α -PB racks (lines), reduces head losses by 60 and 75% for PR and PH bars, respectively. These percentages tend to increase with a decreasing α .

4 Velocity distribution along angled racks with streamwise bars

4.1 Experimental results upstream of α -SB racks

PIV and ADV measurements were carried out for all 18 trashrack configurations. The channel structure made it difficult to obtain useful images in both the upstream and the downstream zones of the rack. Therefore, we focused primarily on the $\alpha = 45^\circ$ configuration (Fig. 3), acquiring images at four locations. PIV results at $\alpha = 30^\circ$ and 60° are consistent with those obtained at $\alpha = 45^\circ$, but are not shown here because they are limited to a restricted area.

Figure 3 shows the velocity map acquired around an α -SB rack with PR bars, where $e = 10$ mm and $\alpha = 45^\circ$. The axial velocity U does not vary significantly and tends to decrease slightly (approximately 10%) towards the downstream end of the rack. Downstream of the rack, velocity maps show a low-velocity zone near the right wall.

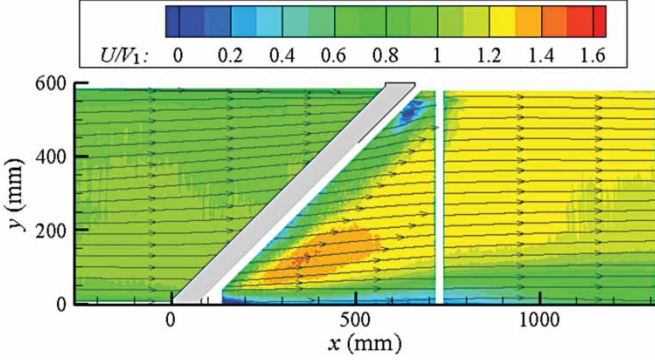


Figure 3 Velocity distribution around α -SB racks with $\alpha = 45^\circ$. U/V_1 fields are calculated from PIV measurements. Bars are rectangular and $e = 10$ mm. The dark blue area at the downstream end of the rack is a zone of poor correlation caused by air bubbles reflecting the laser beam

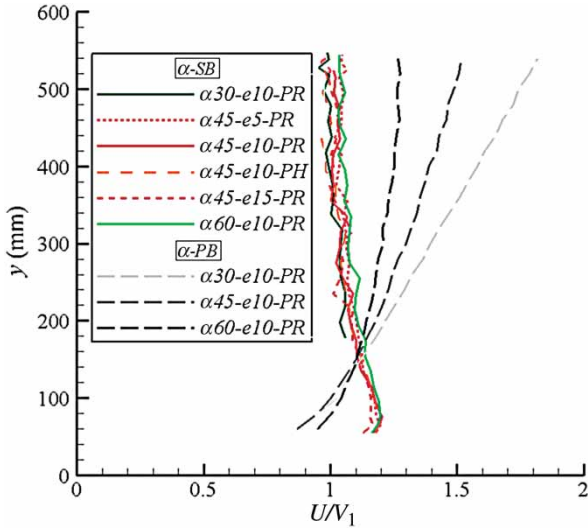


Figure 4 Comparison between velocity distributions obtained by Raynal *et al.* (2013) along α -PB racks with those measured in this study along α -SB racks with various angles α , bar shapes and bar spacings e . Velocities are measured with an ADV probe at 50 mm upstream of the rack. The component U is normalized by the upstream mean velocity V_1

ADV measurements were also carried out in order to complete and confirm the PIV data, especially for $\alpha = 30^\circ$ and 60° . Figure 4 compares the velocity profiles measured along α -SB

racks, 50 mm upstream of the rack, for various rack angles, bar spacings and the two bar shapes. The velocity changes related to bar spacing and bar shape are not significant ($\leq 10\%$). The same holds for α -SB racks with different α values (Fig. 4). In short, for all bar spacings, bar shapes and rack angles, virtually identical streamwise velocity distributions are obtained along the rack, with U ranging from $1.2 V_1$ at $y = 50$ mm ($y/B = 0.08$) to $1.05 V_1$ at $y = 550$ mm ($y/B = 0.92$). This velocity distribution differs from that along α -PB racks where velocities significantly increased as shown in Fig. 4.

4.2 Comparison with α -PB racks and biological criteria

Table 1 compares previous results for α -PB racks with those obtained with α -SB racks in this study. It focuses on V_n and V_t/V_n values and presents the worst values in terms of fish-guidance and impingement criteria, i.e. the maximum V_n and minimum V_t/V_n measured values are presented. For comparison purposes, the table also shows the results using the theoretical values of V_n and V_t calculated by geometrical projection (Eq. 4) and the ratios between the measured and theoretical values

$$V_{t,th} = V_1 \cos(\alpha) \quad V_{n,th} = V_1 \sin(\alpha) \quad \frac{V_{t,th}}{V_{n,th}} = \frac{1}{\tan(\alpha)} \quad (4)$$

The main difference between the two types of rack in Table 1 is the effect of the rack angle. Of course, the V_n and V_t/V_n measured values are modified by the rack angle for both rack types. However, the ratio between the measured and theoretical values does not depend on the rack angle for α -SB racks. Indeed, for all α values, the following equations relate measured values to theoretical ones

$$\left[\frac{V_n}{V_1} \right]_{measured} \approx 1.2 \left[\frac{V_n}{V_1} \right]_{theoretical} = 1.2 \sin(\alpha) \quad (5)$$

$$\left[\frac{V_t}{V_n} \right]_{measured} \approx 0.87 \left[\frac{V_t}{V_n} \right]_{theoretical} = \frac{0.87}{\tan(\alpha)} \quad (6)$$

Equations 5 and 6 make the calculation of fish-friendly angles easier. Because V_t/V_n must be higher than 1 to meet the guidance

Table 1 Maximum normal velocities V_n and minimum tangential to normal velocity ratios V_t/V_n for α -PB and α -SB racks for various α values

	α ($^\circ$)	Max. normal component			Min. tangential to normal velocity ratio		
		V_n/V_1	$V_{n,th}/V_1$	$V_n/V_{n,th}$	V_t/V_n	$V_{t,th}/V_{n,th}$	$[V_t/V_n]/[V_{t,th}/V_{n,th}]$
α -PB	60	1.1	0.87	1.27	0.5	0.58	0.87
	45	1.1	0.71	1.56	0.9	1.0	0.90
	30	1.1	0.5	2.00	1.7	1.73	0.98
α -SB	60	1.0	0.87	1.15	0.5	0.58	0.87
	45	0.85	0.71	1.20	0.87	1.0	0.87
	30	0.6	0.5	1.20	1.5	1.73	0.87

Note: For each parameter, measured values (first column), theoretical values obtained with Eq. 4 (second column) and ratios between measured and theoretical values (third column) are presented.

criterion, Eq. 6 can be used and transformed into Eq. 7

$$\frac{0.87}{\tan(\alpha)} \geq 1 \quad (7)$$

Resolution of Eq. 7 produces the maximum rack angle acceptable for good guidance along the rack. This value is approximately $\alpha = 41^\circ$. Similarly, Eq. 5 can be used to determine the upstream mean velocity range for which the impingement criterion is satisfied. Equation 8 combines the impingement criterion ($V_n \leq 0.5 \text{ ms}^{-1}$) with Eq. 5

$$1.2 \sin(\alpha) V_1 \leq 0.5 \text{ ms}^{-1} \quad (8)$$

Using the maximum α calculated for the guidance criterion, i.e. $\alpha = 41^\circ$, Eq. 8 results in $V_1 \leq 0.64 \text{ ms}^{-1}$. This approach velocity limit is somewhat restrictive in that many hydroelectric power plants operate with higher approach velocities (often between 0.6 and 0.9 ms^{-1}). For higher V_1 values, the angle of α -SB racks must be lower to avoid impingement risks. For instance, for $V_1 = 0.9 \text{ ms}^{-1}$, the rack angle must be $\alpha = 27.5^\circ$.

4.3 Experimental results downstream of α -SB racks and comparison with α -PB racks

Transverse ADV profiles downstream of the rack were measured to analyse the flow distribution as a function of various rack parameters. Because head losses may vary and may affect downstream velocities, the velocity component U is normalized using V_2 instead of V_1 .

Figure 5 compares these profiles along α -SB racks for different configurations. At $\alpha = 45^\circ$, neither the bar shape nor the bar spacing has a significant effect on the velocity profiles, which all comprise a zone, extending from $y = 550 \text{ mm}$ to $y = 185 \text{ mm}$, where velocities are rather constant, and a low-velocity zone at lower y values. On the other hand, the rack angle does influence the size of the low-velocity zone which tends to grow with the decreasing angle α , i.e. increasingly slanted racks. Extension of the low-velocity zone along the y -axis has been estimated at 21, 31 and 37% of the channel width for $\alpha = 60, 45$ and 30° , respectively.

It should be noted that downstream velocities are asymmetrical for the two types of rack and that the low-velocity zones, which can even become an eddying zone for α -PB racks, are located on opposite sides of the channel. Both curves may be decomposed into two distinct parts separated by a large velocity gradient, but this difference between low and high velocities is much larger for α -PB racks. Furthermore, the low-velocity zone extends over approximately 200 mm for α -SB racks compared with approximately 300 mm for α -PB racks.

Another way to analyse the downstream non-uniformity illustrated in Fig. 5 is to calculate the amount of water that flows in each lateral half of the channel, which is a commonly used criterion to assess the quality of the flow at the turbine entrance. In

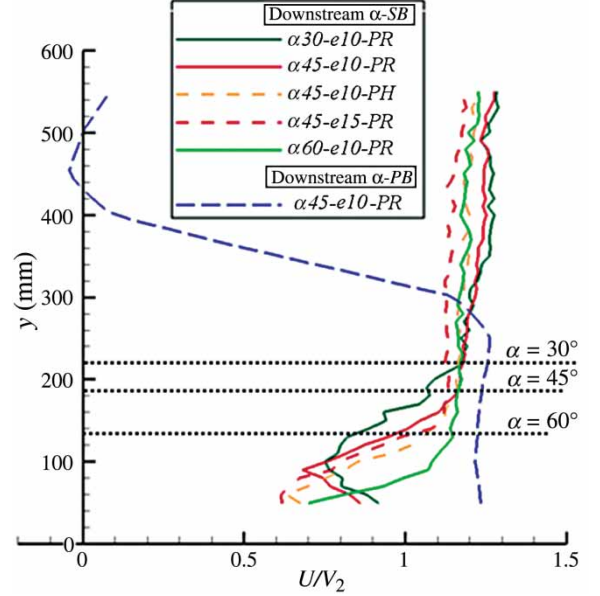


Figure 5 Transverse velocity distributions (ADV at $x = 1 \text{ m}$) downstream of α -SB racks with various angles α , bar shapes and bar spacings e . The width of the low-velocity zone for each rack angle is symbolized by a horizontal dotted line. A profile measured along a α -PB rack (blue line) by Raynal *et al.* (2013) completes the analysis. The component U is normalized by V_2

the present study, this can be achieved by integrating downstream velocity profiles which should provide two surface discharge values (one for each lateral half). Downstream of α -PB racks, 82% of the water flows in the faster lateral half, whereas downstream of α -SB racks, this is the case for only 52–55% of the water. These last figures clearly illustrate the advantage of angled racks with streamwise bars over those with perpendicular bars.

5 Conclusions

This paper focuses on the effect of streamwise bars on angled trashracks. The influences of bar spacing, bar shape and rack angle on head losses and velocity distributions have been investigated.

Head-loss measurements show that ξ depends on the rack angle α between 30° and 60° . Head-loss coefficients of α -SB racks may be predicted using an equation for vertical racks such as Eq. 3, drawn from Raynal *et al.* (2013). Furthermore, head losses for α -SB racks are much lower than those generated by angled racks with perpendicular bars. Setting bars streamwise reduces head losses by 60% for angled racks with $\alpha = 45^\circ$, rectangular bars and a blockage ratio $O_g = 0.39$. This figure increases for more streamlined bars, lower α values and lower blockage ratios.

The velocity distribution upstream of α -SB racks is not significantly influenced by the rack parameters. For all rack angles, bar shapes and bar spacings tested, the axial component slowly decreases along racks from $U = 1.2V_1$ at $y = 0.08B$ to $U = 1.05V_1$ at $y = 0.92B$. This contrasts with α -PB racks for

which U values depend on the rack angle. Moreover, normal and tangential velocities measured along α -SB racks are proportional to theoretical velocities and may be estimated for all α values.

Velocity profiles downstream of α -SB racks highlight the presence of a low-velocity zone. These profiles are not significantly affected by bar shape or bar spacing, however the width of the low-velocity zone tends to increase with a decreasing α value. Compared with α -PB racks, which generate larger asymmetries with eddying flows, α -SB racks better maintain the homogeneity of downstream velocity profiles.

In conclusion, this study estimated the suitability of angled trashracks with streamwise bars for fish-friendly intakes. Head losses generated by angled racks with streamwise bars are much lower than those caused by perpendicular bars. Moreover, the downstream velocity distribution is more homogeneous with α -SB racks. From the biological point of view, fish-guidance and fish-impingement criteria are met when $\alpha = 41^\circ$ and $V_1 \leq 0.64 \text{ ms}^{-1}$. For higher approach velocities V_1 , α must be reduced to prevent fish from being impinged. All these results should assist engineers in designing suitable trashracks for water intakes.

Funding

This work was funded by the European Regional Development Fund, the Région Poitou-Charentes, ONEMA, ADEME, EDF, CNR and SHEM. Their support is greatly appreciated.

Notation

b, b_{ext}	= bar thickness and thickness of the lateral support (m)
B	= channel width (m)
B_g	= trashrack width (m)
D_{sp}	= thickness of the horizontal support (m)
e	= clear space between two bars (m)
H_1, H_2	= upstream and downstream water depths (m)
K_i	= form coefficient in Raynal <i>et al.</i> (2013) head-loss equation (–)
N_b	= number of bars (–)
O_b	= blockage ratio due to bars and lateral supports (–)
O_g	= trashrack-blockage ratio (–)
O_{sp}	= blockage ratio of the transverse elements to the upstream water depth (–)

PR, PH	= bar shape (rectangular and hydrodynamic) (–)
Q	= discharge (ms^{-3})
U, V, W	= velocity components along x, y and z respectively (ms^{-1})
V_1, V_2	= upstream and downstream mean velocities (ms^{-1})
V_t, V_n	= tangential and normal velocity components at the rack face (ms^{-1})
x, y, z	= streamwise, transverse and vertical coordinates (m)
α	= trashrack angle from wall ($^\circ$)
α -PB, α -SB	= abbreviations for angled trashracks with perpendicular and streamwise bars
$\Delta H, \Delta H_0$	= head loss due to the channel and head loss due to the rack (m)
ξ	= trashrack head-loss coefficient (–)

References

- Chatellier, L., Wang, R.W., David, L., Courret, D., Larinier, M. (2011). Experimental characterization of the flow across fish-friendly angled trashrack models. Proc. 34th *IAHR Congress*, Brisbane, 2776–2783.
- Courret, D., Larinier, M. (2008). Guide pour la conception de prises d'eau "ichtyocompatibles" pour les petites centrales hydroélectriques. Report *GHAAPPE RA.08.04.*, Agence de l'environnement et de la maîtrise de l'énergie (ADEME) (www.onema.fr/IMG/pdf/2008_027.pdf).
- Environment Agency. (2012). Hydropower good practice guidelines. Screening requirements (<http://www.environment-agency.gov.uk/business/topics/water/126575.aspx>).
- Kriewitz, C.R., Lucas, J., Lais, A. (2012). Downstream fish migration and intake structure optimization – a synergy? Proc. 2nd *IAHR Europe Congress*, Munich (D8, 6p).
- NMFS. (2011). Anadromous salmonid passage facility design. NMFS, Northwest Region, Portland, Oregon (http://www.nwr.noaa.gov/hydropower/ferc_licensing/non_federal_dams_ferc.html).
- OTA. (1995). Fish passage technologies: Protection at hydropower facilities. Report OTA-ENV-641 (<http://www.fas.org/ota/reports/9519.pdf>).
- Raynal, S., Chatellier, L., Courret, D., Larinier, M., David, L. (2013). An experimental study on fish-friendly trashracks – part 2. Angled trashracks. *J. Hydraulic Res.* 51(1), 67–75.